HIPPOCAMPUS SEGMENTATION THROUGH GRADIENT BASED RELIABILITY MAPS FOR LOCAL BLENDING OF ACM ENERGY TERMS

Dimitrios Zarpalas[1,2], *Polyxeni Gkontra*[1], *Petros Daras*[1], *and Nicos Maglaveras*[1,2], *Senior Member, IEEE*

1: Centre for Research and Technology Hellas

6th Km Charilaou-Thermi rd, 57001, Thessaloniki, Greece. Email: {zarpalas, gkontra, daras}@iti.gr

2: Laboratory of Medical Informatics, Medical School, Aristotle University of Thessaloniki, 54124

Thessaloniki, Greece. Email: nicmag@med.auth.gr

ABSTRACT

This paper presents a novel 3D segmentation framework for structures with spatially varying boundary properties, such as the hippocampus (HC). The proposed method is based on Active Contour Models (ACMs) built on top of the multi-atlas concept. We propose the incorporation of an Adaptive Gradient Distibution on the Boundary map (AGDB) into the ACM framework. AGDB, by being adapted to the evolving contour, constantly redefines, at a voxel level and at each contour evolution, the degree of contribution of the image information and the prior information to the energy minimization. The proposed segmentation scheme was tested for HC segmentation using the publicly available IBSR database.

Index Terms— Hippocampus segmentation, brain MRI, gradient based reliability maps, local blending of ACM energy terms

1. INTRODUCTION

Neurodegenarative disorders cause morphological deformation in various brain structures. Morphological analysis and shape comparisons of brain structures from healthy and diseased subjects can help to detect such deformations, thus leading to possible biomarker identification. The latter is useful in improving diagnosis especially for diseases for which there are only a few diagnostic tools available. Accurate and reliable automatic segmentation of medial temporal lobe structures, such as the hippocampus (HC), is considered a key requirement for the assessment, treatment and follow-up of disorders, for which HC have been found to be influenced [11]. However, it requires overcoming the inherent difficulties of medical imaging, which result in weak or missing boundaries between neighboring structures, such as the challenging case of the borders between HC and the neighboring amygdala (AG), where the imaging resolution is not sufficient to depict it, as Figure 1 shows.

Atlas based segmentation, and especially multi-atlas, is the most appreciated and commonly used concept for per-

Fig. 1. A sagittal slice, highlighting the HC-AG complex. Purple and cyan 3D reconstructions of HC and AG, respectively, are overlayed on the zoomed HC-AG region.

forming multiple structures' segmentation. Many approaches exist in the literature ([18], [13], [14], [8], [15], [3], [2], etc.), which primarily differ on the utilized registration technique, on the fusion strategy of the multiple atlases, and on the selection of the most appropriate atlases. The efficiency of the multi-atlas concept has also been demonstrated in [5], where four different types of segmentation techniques were compared. A recent enhancement of the label propagation concept, on an effort to avoid the inherent computational cost of the non-rigid registrations, is offered by [10], [9], [21] through patch-based approaches for fusing the label images. Attempts have been made to further improve the performance of the multi-atlas concept by offering post-processing steps, which include fusing the multi-atlas concept with intensity classification and nearest neighbor connectivity [22], with intensity modelling [18, 17], or with multi-scale algorithms that use graph representation [1].

Active Contour Models offer another alternative for the task of segmentation. ACMs primarily facilitate (i) edge-based methods, such as the popular Geometric Active Contour model (GAC) [6], which utilizes an edge-stop function to drive the evolution towards edges, and (ii) region-based methods, which use intensities' statistical information, and are more robust on detecting weak edges [7]. However, hybrid approaches, which combine both edge-based and region-based terms into the segmentation framework, tend to be more powerful [27] as they benefit from the properties of both edge-based and region-based terms. ACMs have been further improved for medical image segmentation through the addition

of prior knowledge. A work toward this is the one of Leventon et al. in [16] who combined the GAC model with statistical information about the shapes undergoing segmentation. Yang et al. [24], extended Leventon's idea and included a notion of neighborhood prior along with the shape prior, to segment multiple neighboring structures, and incorporated it into the model described in [7]. Recent advances on the ACM method include selective local or global segmentation [28], spatially-varying regularization weights [20], non-linear shape models produced using manifold learning techniques [12], etc.

In this work, we are proposing the incorporation of multi-atlas based prior knowledge on an ACM framework for the task of hippocampus segmentation. The ACM is simultaneously evolved on the target image, an image demonstrating the regions of grey matter tissue, and the spatial distribution map, extracted by the multi-atlas methodology. The energy minimization criterion thus encloses image terms (i.e. how well the contour fits the image) and the prior term (i.e. the likelihood of the enclosed voxels belonging to the hippocampus). More importantly, this method differs from previous relevant attempts, by blending the image terms in a local and adaptive way, within each contour evolution iteration. Previous solutions incorporated their prior term in a global way, neglecting the anatomically varying boundary properties of the structures. In an effort to tackle this shortcoming, we initially proposed balancing image and prior information through a static local weighting map, based on Gradient Distribution on the hippocampus' Boundary (GDB) [25], which was later extended in [26] to become Adaptive (AGDB), based on the evolving contour. This idea was inspired by the fact that a static map could not serve in full extend the variability of the hippocampus' shape. This concept was successfully evaluated on the central sagittal slices of hippocampus. We hereby carefully take into consideration the varying boundary properties of HC, by introducing two more energy terms, and verify the usefullness of this concept on the full 3D HC segmentation on the well known IBSR dataset.

2. PROPOSED METHOD

In a nutshell, the proposed method is an ACM method on top of the multi-atlas concept. The ACM optimization includes four energy terms. The first three are image terms, while the fourth term is the prior term. The image terms are divided to edge-based and region-based. The role of the edge-based, is to guide segmentation towards apparent boundaries, while the role of the region terms is to take lead on regions with weak boundaries. There are two region terms, one based on the initial image information that takes into consideration regional intensity statistics, only around the HC region, and a second that is based on a smoothed image depicting the grey matter tissue, which in turn takes into account whole brain statistics. The prior term is based on the Spatial Distribution Map (SDM), derived by the multi-atlas methodology, and is used

to constraint the evolution on the HG regions with missing borders (i.e. between HC and AG).

$AGDB$'s role is the blending at a voxel level of the three image terms with the prior term in order to accommodate the spatially varying properties of HC's evolving boundary and to aid the evolution process according to the dominant property at that voxel, i.e. image or prior information. This means that $AGDB$ is a weighting map that has equal dimensions with the image and refers to the evolving contour at time step t ($AGDB_t$). $AGDB$ up-weights the image terms in parts of the evolving contour that demonstrate sufficient image information (either strong or weak boundaries). Vice versa, $AGDB$ passes gradually the control of the contour evolution to the prior term in case of insufficient image information by up-weighting the contribution of the prior term. It is initially defined by the density of the gradient values around and on the mean hippocampal shape extracted from a training set. Subsequently, the constructed $AGDB$ is being adapted to the evolving contour by being transformed to the space of the latter, imitating even more the human segmentation way.

2.1. Energy formulation of the model

According to the level set method [19], an evolving curve C in the image domain $\Omega \in R^3$ can be represented implicitly as the zero level set of a Lipschitz function $\phi : R^3 \to \Omega$, $C = \{\mathbf{v} \in \Omega \mid \phi(\mathbf{v}) = 0\}$, where $\mathbf{v} \in \Omega$, $\mathbf{v} = (x, y, z)$ are the coordinates of a voxel and the embedding function ϕ is a signed distance function.

Using AGDB to blend the image terms and the prior term, the energy functional to be minimized in order to drive the evolution of C is defined by:

$$E = E_I(AGDB) + E_{Pr}(\mathbf{1} - AGDB)$$

where $\mathbf{1}$ denotes a matrix of ones, E_I stands for the image terms and E_{Pr} indicates the prior term. E_I refers to the sum of three image terms:

(i) E_{I1}, the edge-based term defined using [6], augmented by a local weighting map M, of same size as the target image I:

$$E_{I1}(M) = \int_{\Omega} M(\mathbf{v})g(\mathbf{v})|\nabla\phi(\mathbf{v})|d\mathbf{v}$$

where g is an edge stopping function [6].

(ii) E_{I2}, the region-based term formulated as in [7]:

$$E_{I2}(M) = \lambda_1^I \int_{\Omega_1} M(\mathbf{v})|I(\mathbf{v})-c_1^I|^2 d\mathbf{v} + \lambda_2^I \int_{\Omega_2} M(\mathbf{v})|I(\mathbf{v})-c_2^I|^2 d\mathbf{v}$$

where c_1^I, c_2^I are the average intensities of I in the region inside Ω_1 and outside Ω_2 the evolving curve, respectively, and λ_1^I, λ_2^I are balancing factors between the properties of the two regions.

(iii) E_{I3}, the region-based term taking into account the tissue type information, extracted by FAST[1]:

$$E_{I3}(M) = \lambda_1^G \int_{\Omega_1} M(\mathbf{v})|G(\mathbf{v})-c_1^G|^2 d\mathbf{v} + \lambda_2^G \int_{\Omega_2} M(\mathbf{v})|G(\mathbf{v})-c_2^G|^2 d\mathbf{v}$$

---

[1] http://www.fmrib.ox.ac.uk/fsl/

where G is a smoothed version of a binary image indicating the regions of I where the gray matter is distributed.

To formulate the prior term (E_{Pr}), the training set is non-rigidly registered to the target image, using the symmetric normalization methodology (SyN) [4] provided by the ANTs toolkit. The spatial distribution map (L) is then defined by the use of a weighted fusion scheme, where the weights indicate the normalized cross-correlation between each training image and the target image. Given L, the prior term is also created using the [7] approach, since L is an image with smooth transitions:

$$E_{Pr}(M) = \lambda_1^L \int_{\Omega_1} M(\mathbf{v})|L(\mathbf{v})-c_1^L|^2 d\mathbf{v} + \lambda_2^L \int_{\Omega_2} M(\mathbf{v})|L(\mathbf{v})-c_2^L|^2 d\mathbf{v}$$

Combining the above equations and using the level set framework, the evolution equation becomes:

$$\frac{\vartheta\phi}{\vartheta t} = AGDB_t \circ \left[\frac{\vartheta\phi_{I1}}{\vartheta t} + \frac{\vartheta\phi_{I2}}{\vartheta t} + \frac{\vartheta\phi_{I3}}{\vartheta t}\right] + (\mathbf{1} - AGDB_t) \circ \frac{\vartheta\phi_{Pr}}{\vartheta t}$$

$$= AGDB_t \circ \left[g|\nabla(\phi)|\mathrm{div}(\frac{\nabla\phi}{|\nabla\phi|}) + \nabla g \cdot \nabla\phi\right] +$$

$$+ \delta_\epsilon(\phi)\left[\mu\,\mathrm{div}\left(\frac{\nabla\phi}{|\nabla\phi|}\right) - \nu -\right.$$

$$- AGDB_t \circ \left(\lambda_1^I(I-c_1^I)^2 - \lambda_2^I(I-c_2^I)^2\right) -$$

$$- AGDB_t \circ \left(\lambda_1^G(G-c_1^G)^2 - \lambda_2^G(G-c_2^G)^2\right) -$$

$$\left.- (\mathbf{1} - AGDB_t) \circ \left(\lambda_1^L(L-c_1^L)^2 - \lambda_2^L(L-c_2^L)^2\right)\right]$$

where $\mu\,\mathrm{div}\left(\frac{\nabla\phi}{|\nabla\phi|}\right)$ is a regularization term that controls the degree of smoothness; ν controls the propagation speed; α is the balloon force that controls the contour's contraction or expansion; $\delta_\epsilon(\phi)$ is the dirac function and $\circ$ operation denotes the Hadamard product.

2.2. Building AGDB

An initial AGDB ($AGDB_{init}$) must be calculated to construct the local weighting map $AGDB_t$ that refers to an evolving contour ϕ_t at each iteration t. In this respect, a four-step procedure is followed. Firstly, the corresponding level set function Φ_i is constructed for every registered training image B_i, $i = 1, \ldots, N$. Averaging them, the mean level set is defined by $\overline{\Phi} = \frac{1}{N}\sum \Phi_i$. Secondly, the canny edge detector is applied for every B_i, producing C_i. The advantage of using canny is that it detects both strong and weak edges, thus accommodates all image terms (i.e. strong edges for edge-based and weak edges for region-based terms respectively). Thirdly, the intersection between the zero level set of $\Phi_i, i = 1, ..., N$ and the dilated version of image C_i is defined, resulting in D_i. Lastly, $AGDB_{init}$ is produced with the application of the same fusion scheme on D_i, as the one used to calculate L.

Following the construction of $AGDB_{init}$, $AGDB_t$ is subsequently defined by mapping $AGDB_{init}$ to the space of the evolving contour ϕ_t. This way the weighting map is more able to accommodate the varying image properties around the evolving boundary. $\overline{\Phi}$ and the evolving contour ϕ_t are therefore first transformed into binary masks M_1, M_2. M_1 is then non-rigidly registered to M_2. The resulting transformation is applied on $AGDB_{init}$ to transfer it to the space of ϕ_t, thus producing $AGDB_t$.

3. EXPERIMENTAL RESULTS AND DISCUSSION

The proposed method was evaluated using the IBSR dataset, provided by the center for Morphometric Analysis at the Massachusetts General Hospital[2], which contains T1-weighted image volumes from 18 subjects and their corresponding manual segmentations.

A leave-one-out procedure was undertaken for all subjects. Figure 2 offers segmentation results of three subjects, along with 3D reconstructions of the estimated volumes, where one can see the high amount of agreement between the extracted volumes and the ground truth.

To further assess the performance of the $AGDB$-based method, the segmentation results were also compared against previously published results on the same dataset, of various methods. The mean Dice coefficient was used as it was available for all methods in their original manuscripts. The result of a straightforward multi-atlas fusion scheme based on the ANTs registration is also calculated. The resulting evidence is provided in Table 1, which demonstrate the enhanced accuracy of the proposed method, yielding the higher Dice value compared to all other methods. As it can be seen, the proposed AGDB-based ACM scheme on top of the ANTs multi-atlas, offers an increase in accuracy of the exact same amount for the task of HC segmentation, with the one of [18], where intensity modelling through expectation maximization was used on top of their multi-atlas implementation. However, as the registration techniques increase their performance, the potential space for further increase narrows, as it reaches the upper limit of inter-rater variability. Further, the results verify the similar behaviour of the ANTs-based multi-atlas with the patch-based method of Rousseau et al., as can be seen in [21]. Please note that the efforts of Rousseau et al. are primarily on increasing the execution performance, rather than the segmentation accuracy. Thus, replacing the non-rigid registration steps of our method with the patch-based approach proposed by [21] will potentially lead to same accuracy improvement with reduced computational cost.

Concluding, the proposed $AGDB$-based HC segmentation framework, takes carefully into account and models appropriately the spatially varying boundary properties of HC. The constant adaptation of $AGDB$ to the evolving contour mimics the human understanding of region properties. Furthermore, using the multi-atlas concept to build the spatial distribution map L and the $AGDB_{init}$, subject-specific information is incorporated into the segmentation framework.

---

[2]http://www.cma.mgh.harvard.edu/ibsr/
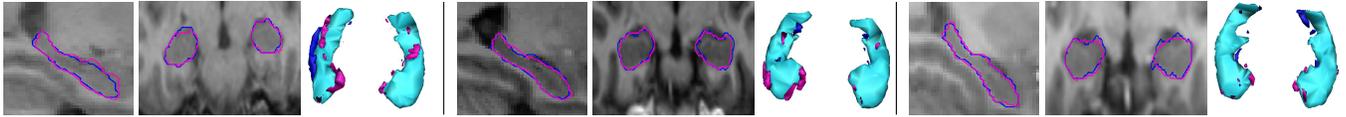
Fig. 2. Segmentation results on a sagittal and an axial slice and the corresponding 3D reconstructions for subjects 6, 9, 14. Pink on the 2D slices shows the manual segmentation, whilst blue the AGDB result. For the 3D reconstructions, cyan indicates True Positive voxels, blue the False Positives, and pink the False Negatives.

Method	HC	Method Description
AGDB	**0.84**	$AGDB$-based ACM on top of multi-atlas
ANTs [4]	0.83	Multi-atlas based on the ANTs toolkit
Method in [21]	0.83	Patch-based labelling
Method in [18]	0.81	Multi-atlas & Expectation Maximization
Method in [22]	0.81	Multi-atlas & accuracy weighted vote
Method in [15]	0.76	Registration & supervised atlas correction
Method in [3]	0.75	Multi-atlas & multiple combination strategies
Method in [23]	0.75	FreeSurfer
Method in [1]	0.69	Multiscale segm. with probabilistic atlas

Table 1. Mean Dice similarity coefficient for evaluating the performance of the proposed method against other segmentation approaches tested in IBSR dataset.

On the widely used IBSR dataset, it yielded the best results when compared with other state-of-the-art methods, proving the proposed concept's efficacy and accuracy.

4. REFERENCES

[1] A. Akselrod-Ballin, M. Galun, J.M. Gomori, A. Brandt, R. Basri, "Prior knowledge driven multiscale segmentation of brain MRI", Medical Image Computing and Computer-Assisted Intervention, 2007.

[2] P. Aljabar, R.A. Heckemann, A. Hammers, J.V. Hajnal, D. Rueckert, "Multi-atlas based segmentation of brain images: atlas selection and its effect on accuracy", NeuroImage, vol. 46, pp. 726-738, 2009.

[3] X. Artaechevarria, A. Munoz-Barrutia, C. Ortiz-de-Solorzano, "Combination strategies in multi-atlas image segmentation: Application to brain MR data", IEEE Trans. Med. Imag., vol. 28(8), 2009.

[4] B.B. Avants, C.L Epstein, M. Grossman, J.C. Gee, "Symmetric diffeomorphic image registration with cross-correlation: Evaluating automated labeling of elderly and neurodegenerative brain", Med. Image Anal., vol. 12(1), pp. 26-41, 2008.

[5] K.O. Babalola, B. Patenaude, P. Aljabar, J. Schnabel, D. Kennedy, W. Crum, S Smith, T.F. Cootes, M. Jenkinson, D. Rueckert, "Comparison and evaluation of segmentation techniques for subcortical structures in brain MRI", Med. Image Comput. Comput. Assist Interv., 2008.

[6] V. Caselles, R. Kimmel, G. Sapiro, "Geodesic active contours", International Journal of Computer Vision, vol. 22(1), pp. 61-79, 1997.

[7] T. Chan and L. Vese, "Active contours without edges", IEEE Trans. Med. Imag., vol. 10, pp. 266-277, 2001.

[8] D.L. Collins and J.C. Preussner, "Towards accurate, automatic segmentation of the hippocampus and amygdala from MRI by augmenting ANIMAL with a template library and label fusion", NeuroImage, vol. 52(4), pp. 1355-1366, 2010.

[9] P. Coupé, J. Manjón, V. Fonov, J. Pruessner, M. Robles, D.L. Collins, "Nonlocal Patch-based label fusion for Hippocampus Segmentation", International Conference on Medical Image Computing and Computer Assisted Intervention (MICCAI), LNCS 6363, pp. 129-136, 2010.

[10] P. Coupé, J. Manjón, V. Fonov, J. Pruessner, M. Robles, D.L. Collins, "Patch-based Segmentation using Expert Priors: Application to Hippocampus and Ventricle Segmenatation", NeuroImage, 2011.

[11] N.A. DeCarolis, A.J. Eisch, "Hippocampal neurogenesis as a target for the treatment of mental illness: a critical evaluation", Neuropharmacology, vol. 58(6), pp.884-93, 2010.

[12] P. Etyngier, F. Ségonne, R. Keriven, "Active-Contour-Based Image Segmentation Using Machine Learning Techniques", International Conference on Medical Image Computing and Computer Assisted Intervention (MICCAI), pp. 891-899, 2007.

[13] R.A. Heckemann, J.V. Hajnal, P. Aljabar, D. Rueckert, A. Hammers, "Automatic anatomical brain MRI segmentation combining label propagation and decision fusion", NeuroImage, vol. 33(1), pp. 115-126, 2006.

[14] A.R. Khan, N. Cherbuin, W. Wen, K.J. Anstey, P. Sachdev, M.F. Beg,"Optimal weights for local multi-atlas fusion using supervised learning and dynamic information (SuprDyn): Validation on hippocampus segmentation", NeuroImage, vol. 56, pp. 126-139, 2011.

[15] A.R. Khan, M.K. Chung, M.F. Beg, "Robust atlas-based brain segmentation using multi-structure confidence-weighted registration", Medical Image Computing and Computer-Assisted Intervention (MICCAI), LNCS 5762, pp. 549 -557, 2009.

[16] J. M. Leventon, E. Grimson, O. Faugeras, "Statistical shape influence in geodesic active contours", IEEE Conference on Computer Vision Pattern Recognition, vol. 1, pp. 316-323, 2000.

[17] F. van der Lijn, T. den Heijer, M.M.B. Breteler, W.J. Niessen, "Hippocampus segmentation in MR images using atlas registration, voxel classification, and graph cuts", NeuroImage, 2008.

[18] J.M. Lötjönen, R. Wolz, J.R. Koikkalainen, L. Thurfjell, G. Waldemar, H. Soininen, D. Rueckert, "Fast and robust multi-atlas segmentation of brain magnetic resonance images", Neuroimage, 2010.

[19] S. Osher, R. Fedkiw, "Level Set Methods and Dynamic Implicit Surfaces", Springer Verlag, 2002.

[20] J. Rao, R. Abugharbieh, G. Hamarneh, "Adaptive Regularization for Image Segmentation Using Local Image Curvature Cues. European Conference on Computer Vision (ECCV), 2010.

[21] F. Rousseau, P.A. Habas, C. Studholme, "A supervised patch-based approach for human brain labeling", IEEE Trans. Med. Imag., 2011.

[22] M. Sdika, "Combining atlas based segmentation and intensity classification with nearest neighbor transform and accuracy weighted vote", Med. Image Anal., vol. 14(2), pp. 219-226, 2010.

[23] B. Fischl, D.H. Salat, E. Busa, M. Albert, M. Dieterich, C. Haselgrove, A. van der Kouwe, R. Killiany, D. Kennedy, S. Klaveness, A. Montillo, N. Makris, B. Rosen, A.M. Dale, "Whole brain segmentation: Automated labeling of neuroanatomical structures in the human brain", Neuron, vol. 33(3), pp. 341 -355, 2002.

[24] J. Yang, L.H. Staib and J.S. Duncan, "Neighbor-Constrained Segmentation with Level Set Based 3D Deformable Models", IEEE Trans. Med. Imag., vol. 23(8), pp. 940-8, 2004.

[25] D. Zarpalas, A. Zafeiropoulos, P. Daras, N. Maglaveras, "Hippocampus Segmentation using a Local Prior Model on its Boundary", Inter. Conf. on Machine Vision, Image Processing and Pattern Analysis, 2011.

[26] D. Zarpalas, P. Gkontra, P. Daras, N. Maglaveras, "Segmentation through a local and adaptive weighting scheme, for contour-based blending of image and prior information", The 25th IEEE International Symposium on Computer-Based Medical Systems (CBMS), 2012

[27] Y. Zhang, B.J. Matuszewski, L.-K. Shark, C.J. Moore, "Medical Image Segmentation Using New Hybrid Level-Set Method", Fifth International Conference BioMedical Visualization: Information Visualization in Medical and Biomedical Informatics, pp. 71-76, 2008.

[28] K. Zhang, L. Zhang, H. Song, W. Zhou, "Active contours with selective local or global segmentation: A new formulation and level set method", Image and Vision Computing, vol. 28(4), pp. 668-6, 2010.